














Analysis of SARS-CoV-2 mutations in Mexico, Belize, and isolated regions of Guatemala and its implication in the diagnosis

María Teresa Hernández-Huerta PhD¹  | Laura Pérez-Campos Mayoral PhD²  |
 Carlos Romero Díaz PhD²  | Margarito Martínez Cruz PhD³  |
 Gabriel Mayoral-Andrade PhD²  | Luis Manuel Sánchez Navarro⁴  |
 María Del Socorro Pina-Canseco PhD²  | Eli Cruz Parada³ |
 Ruth Martínez Cruz PhD²  | Eduardo Pérez-Campos Mayoral PhD²  |
 Alma Dolores Pérez Santiago PhD³  | Gabriela Vásquez Martínez PhD³  |
 Eduardo Pérez-Campos PhD^{2,3,5}  | Carlos Alberto Matias-Cervantes PhD¹ 

¹CONACyT Facultad de Medicina y Cirugía, Universidad Autónoma "Benito Juárez" de Oaxaca, Oaxaca, Mexico

²Centro de Investigación Facultad de Medicina UNAM-UABJO, Facultad de Medicina y Cirugía, Universidad Autónoma "Benito Juárez" de Oaxaca, Oaxaca, Mexico

³Tecnológico Nacional de México/IT de Oaxaca, Oaxaca, Mexico

⁴Facultad de Medicina y Cirugía, Universidad Autónoma "Benito Juárez" de Oaxaca, Oaxaca, Mexico

⁵Laboratorio de Patología Clínica "Dr. Eduardo Pérez Ortega", Oaxaca, Mexico

Correspondence

Eduardo Pérez-Campos, Tecnológico Nacional de México/IT de Oaxaca, 68030 Oaxaca, México.

Email: perezcampos@prodigy.net.mx

Carlos Alberto Matias-Cervantes, CONACyT Facultad de Medicina y Cirugía, Universidad Autónoma "Benito Juárez" de Oaxaca, 68020 Oaxaca, México.

Email: carloscervantes.ox@outlook.com

Abstract

The genomic sequences of severe acute respiratory syndrome coronavirus 2 (SARS-CoV-2) worldwide are publicly available and are derived from studies due to the increase in the number of cases. The importance of study of mutations is related to the possible virulence and diagnosis of SARS-CoV-2. To identify circulating mutations present in SARS-CoV-2 genomic sequences in Mexico, Belize, and Guatemala to find out if the same strain spread to the south, and analyze the specificity of the primers used for diagnosis in these samples. Twenty three complete SARS-CoV-2 genomic sequences, available in the GISAID database from May 8 to September 11, 2020 were analyzed and aligned versus the genomic sequence reported in Wuhan, China (NC_045512.2), using Clustal Omega. Open reading frames were translated using the ExpASy Translate Tool and UCSF Chimera (v.1.12) for amino acid substitutions analysis. Finally, the sequences were aligned versus primers used in the diagnosis of COVID-19. One hundred and eighty seven distinct variants were identified, of which 102 are missense, 66 synonymous and 19 noncoding. P4715L and P5828L substitutions in replicase polyprotein were found, as well as D614G in spike protein and L84S in ORF8 in Mexico, Belize, and Guatemala. The primers design by CDC of United States showed a positive *E* value. The genomic sequences of SARS-CoV-2 in Mexico, Belize, and Guatemala present similar mutations related to a virulent strain of greater infectivity, which could mean a greater capacity for inclusion in the host genome and be related to an increased spread of the virus in these countries, furthermore, its diagnosis would be affected.

KEYWORDS

genetic variation, mutations, SARS coronavirus

1 | INTRODUCTION

The first cases of severe acute respiratory syndrome coronavirus 2 (SARS-CoV-2) were reported in December 2019 in Wuhan city, Hubei province, China^{1,2}; thus initiating the coronavirus pandemic (COVID-19).³ According to the information released from scientists around the world and the GISAID consortium, until September 15, 2020, SARS-CoV-2 has caused 29,445,572 cases worldwide and 931,454 deaths.⁴ According to predictions,⁵ the total number of deaths will increase to 2,778,330 by January 1, 2021.

To identify how the virus spread, cross-sectional studies with phylogenetic analysis and markers that identified mutations were implemented.⁶ It is known from epidemiological reports that the first cases started in Mexico from the East, particularly from the United States, Spain, France, Germany, Singapore, and especially from Bergamo, Italy.^{7,8} In addition, we think that the dispersion went from Mexico to Belize and Guatemala, and therefore, there could be the same molecular characteristics, for this reason we included these three countries in our study.

SARS-CoV-2 is closely related to the SARS-CoV and the Middle East respiratory syndrome coronavirus.⁹ Its structure contains a single-stranded RNA (ssRNA) genome with a length of 29,903 bp. It comprised of a 5'-untranslated region (5'-UTR), a conserved replicase domain (ORF1ab) cleaved into 16 nonstructural proteins (NSPs) that participate in virus transcription and genome replication, four structural proteins (S, E, M, and N), several accessory proteins (ORF3a, ORF6, ORF7a, ORF7b, ORF8, and ORF10), and a highly conserved 3'-UTR^{10,11} (Table 1) among other coronaviruses.^{12,13}

The ORF1ab gene encodes for replicase polyprotein 1ab (pp1ab), which is constituted of NSPs (NSP1, NSP2...NSP16). Of these, NSP12 corresponds to RNA-dependent RNA polymerase (RdRp) and is formed by 932 amino acids (4392–5324 residues). The spike (S) protein has been described as responsible for the interaction with the human receptor angiotensin-converting enzyme 2 (hACE2)¹⁴; it is constituted of two domains, the S1 domain, responsible for binding, and the S2 domain that mediates the fusion of the viral and cellular membrane.¹⁵ Moreover, S1 has variations but S2 is highly conserved.¹⁶

Nonsynonymous substitution changes the protein sequences, these have been reported in SARS-CoV-2 in the functional domains of ORF3a.¹⁷ Issa et al.¹⁷ reported that these substitutions are related to virulence, infectivity, ion channel formation, and virus release. ORF3a mutations have been found in other countries such as India.¹⁸

We analyze and identify the characteristics of circulating SARS-CoV-2 mutations present in genomic sequences in Mexico, Belize, and Guatemala, to find out if they have the same molecular characteristics, we also evaluate how these mutations affect the primer design for reverse transcription-polymerase chain reaction (RT-PCR) from the Center for Disease Control and Prevention of the United States (CDC US), CDC China, Charité (Germany), Hong Kong University, and the National Institute of Infectious Diseases (Japan). The results indicated the presence of similar mutations in ORF1ab, S

(S1, S2 or S2'), ORF 3a, ORF7a, ORF8, and N, as well as in the noncoding (5'-UTR and 3'-UTR) and intergenic regions (between ORF3a and E gene) in strains from Mexico, Belize, and Guatemala. Also, we found that primers from the Center for Disease Control and Prevention (CDC US) could present low specificity.

2 | METHODS

We analyzed 457 SARS-CoV-2 genomic sequences from Mexico, Belize, and Guatemala available in the GISAID database (<https://www.gisaid.org/>) from May 8 until September 11, 2020. Of these, we only selected the complete sequences with approximately 29,800–29,900 base pairs (bp); 23 from Mexico (EPI_ISL_426362, EPI_ISL_424667, EPI_ISL_455456, EPI_ISL_426364, EPI_ISL_426363, EPI_ISL_424670, EPI_ISL_424673, EPI_ISL_516613, EPI_ISL_516620, EPI_ISL_454555, EPI_ISL_412972, EPI_ISL_452139, EPI_ISL_424672, EPI_ISL_516625, EPI_ISL_424626, EPI_ISL_455434, EPI_ISL_516609, EPI_ISL_496369, EPI_ISL_493348, EPI_ISL_493336, EPI_ISL_516611, EPI_ISL_455438, and EPI_ISL_496374), four from Belize (EPI_ISL_509713, EPI_ISL_509714, EPI_ISL_509712, and EPI_ISL_509711), and 10 from Guatemala (EPI_ISL_509710, EPI_ISL_509700, EPI_ISL_509699, EPI_ISL_509696, EPI_ISL_509695, EPI_ISL_509702, EPI_ISL_509703, EPI_ISL_509697, EPI_ISL_509698, and EPI_ISL_509701).

Genomic alignments were performed using Clustal Omega (<https://www.ebi.ac.uk/Tools/msa/clustalo/>) versus the SARS-CoV-2 genomic sequence reported from Wuhan, China (NCBI accession number NC_045512.2) as reference. Open reading frames (ORFs) containing the identified variants were translated using the Expasy Translate Tool (<https://web.expasy.org/translate/>) using standard code. Variants and their amino acids were used to create a table of variants (Table 2).

The amino acids corresponding to mutations D614G in the spike protein, P4715L in RdRp, and L84S in ORF8 protein were replaced by Visual Molecular Dynamics (VMD) v.1.9.1 (<https://www.ks.uiuc.edu/>) and visualized with Chimera v. 1.1.12 (<https://www.cgl.ucsf.edu/chimera/>), taking as templates structures from Protein the Data Bank (PDB) proposed by Zhang et al.¹⁹ For the spike protein, we used 6VSB.pdb, which corresponds to the trimeric protein in open conformation that includes the S1 and S2 subdomains²⁰ while for the RdRp, we took chain A of 6M71.pdb reported by Gao et al.²¹

As of September 09, 2020, the crystallographic structure of the ORF8 protein has not been reported, thus we take the one proposed by the Iterative Threading Assembly Refinement (I-TASSER) server²² (QHD43422.pdb). Also, in Mexico, the Berlin test with four oligonucleotides for the RdRp gene (GTGARATGGTCATGTGTGGCGG, FAM-CAGGTGGAACCTCATCAGGAGATGC-BBQ, FAM-CCAGGTGGWACRTCATCMGGTGATGC-BBQ, CARATGTTAAASACTATTAGCATA), three for the E gene (ACAGGTACGTTAATAGTTAATAGCGT, FAM-ACACTAGCCATCCTTACTGCGCTTCG-BBQ, ATATTGCAGCAGTACGCACACA) and three for the N gene (CACATTGGCACCCGCAATC, FAM-ACTTCCTCAAGGAACAACATTGCCA-BBQ, GAGA ACGAGAAGAGGCTTG)²³ are the reference in the Institute of Epidemiological Diagnosis and Reference “Dr. Manuel Martínez Báez”

TABLE 1 Genomic structure of SARS-CoV-2

Gene		ORF1ab	ORF1a	S	ORF3a	E	M	ORF7b	ORF7a	ORF8	N	ORF10	3'-UTR
CDS (bp)	265	21291	13218	3822	828	228	669	132	366	366	1260	117	229
Protein	Noncoding sequence	Replicase poly-protein 1ab	Replicase poly-protein 1a	Spike glycoprotein	Protein 3a	Envelope small membrane protein	Membrane protein	Protein non-structural 7b	Protein 7a	Nonstructural protein8	Nucleo-protein	ORF10 protein	Noncoding sequence
Amino acids	-	7096	4405	1273	275	75	222	43	121	121	419	38	-
Molecular weight (Da)	-	794,058	489,989	141,178	31,123	8365	25,147	5180	13,744	13,831	45,626	4449	-
Function ^a	Regulate the folding, processing of viral RNA	Transcription and replication of viral RNA, RNA-directed RNA polymerase	Transcription and replication of viral RNA-binding and thiol protease	Host-virus interaction and virulence	Modulate virus release	Virus morphogenesis and assembly apoptosis	Host-virus interaction and viral immunoreaction, interactions with other viral proteins	Transmembrane helix	Modulation of host cell cycle by virus	Host-virus interaction	Packages viral genome RNA into a helical ribonucleoprotein (RNP), assembly and interactions with genome and membrane protein M	Unknown function	Unknown function
ID ³	Protein	Y- P_009-72438-9.1	Y- P_009-72529-5.1	Y- P_009-72439-0.1	Y- P_009-72439-1.1	Y- P_009-72439-2.1	Y- P_009-72439-3.1	Y- P_009-72531-8.1	Y- P_009-72439-5.1	Y- P_009-72439-6.1	Y- P_009-72439-7.2	Y- P_009-72439-7.2	

^aNCBI reference sequence: NC_045512.2.

TABLE 2 Nucleotide variants and amino acid substitutions in SARS-CoV-2 genomes in Mexico

ID Mexico	Nucleotide change	Synonymous/nonsynonymous	Position genome	Amino acid substitution	Position protein	Gene	Product
EPI_ISL426362	C>T	Synonymous	8782	S	2839	ORF1ab	NSP4
	T>A	Nonsynonymous	9477	F>Y	3071	ORF1ab	NSP4
	C>T	Synonymous	14805	Y	4847	ORF1ab	NSP10
	C>T	Synonymous	23280	I	573	S	S1
	G>T	Nonsynonymous	25979	G>V	196	ORF3a	3A protein
	C>T	Synonymous	28657	D	128	N	N
	C>T	Nonsynonymous	28863	S>L	197	N	N
	T>C	Nonsynonymous	28144	L>S	84	ORF8	ORF8b protein
	T>C	-	26232	-	-	Intergenic	-
EPI_ISL_424667	C>T	Synonymous	8782	S	2839	ORF1ab	NSP4
	C>T	Synonymous	17470	L	17470	ORF1ab	Helicase
	C>T	Synonymous	26088	I	232	ORF3a	3a Protein
	T>C	Nonsynonymous	28144	L>S	84	ORF8	ORF8b protein
EPI_ISL_455456	C>T	Synonymous	26088	I	232	ORF3a	3a Protein
	T>C	Nonsynonymous	28144	L>S	84	ORF8	ORF8b protein
	C>T	Synonymous	8782	S	2839	ORF1ab	NSP4
EPI_ISL_426364	C>T	Synonymous	8782	S	2839	ORF1ab	NSP4
	C>T	Nonsynonymous	17747	P>L	5828	ORF1ab	Helicase
	A>G	Nonsynonymous	17858	Y>C	5865	ORF1ab	Helicase
	C>T	Synonymous	18060	L	5932	ORF1ab	3'-5' Exonuclease
	C>T	Nonsynonymous	21707	H>Y	49	S	S1
	C>T	Synonymous	23422	V	620	S	S1
	A>T	Synonymous	24694	G	1044	S	S2'
	T>C	Nonsynonymous	28144	L>S	84	ORF8	ORF8b protein
EPI_ISL_426363	C>T	Nonsynonymous	21707	H>Y	49	S	S1
	T>C	Nonsynonymous	28144	L>S	84	ORF8	ORF8b protein
	C>T	Synonymous	23422	V	620	S	S1
	A>T	Synonymous	24694	G	1044	S	S2'
	C>T	Synonymous	8782	S	2839	ORF1ab	NSP4
	C>T	Nonsynonymous	17747	P>L	5828	ORF1ab	Helicase
	A>G	Nonsynonymous	17858	Y>C	5865	ORF1ab	Helicase
	C>T	Synonymous	18060	L	5932	ORF1ab	3'-5' Exonuclease
EPI_ISL_424670	T>C	Nonsynonymous	28144	L>S	84	ORF8	ORF8B protein
	C>T	Synonymous	26088	I	232	ORF3a	3A protein
	C>T	Synonymous	8782	S	2839	ORF1ab	NSP4
EPI_ISL_424673	C>T	Nonsynonymous	936	T>I	224	ORF1ab	NSP2
	C>T	Synonymous	8782	S	2839	ORF1ab	NSP4
	G>T	Nonsynonymous	11083	L>F	3606	ORF1ab	NSP6
	C>T	Nonsynonymous	17747	P>L	5828	ORF1ab	Helicase
	A>G	Nonsynonymous	17858	Y>C	5865	ORF1ab	Helicase
	C>T	Synonymous	18060	L	5932	ORF1ab	3'-5' Exonuclease
	A>T	Synonymous	24694	G	1044	S	S2'
	T>C	Nonsynonymous	28144	L>S	84	ORF8	ORF8b protein
	G>T	Nonsynonymous	28812	S>I	180	N	N
EPI_ISL_516613	C>T	-	241	-	-	5'-UTR	-
	C>T	Nonsynonymous	27964	S>L	24	ORF8	ORF8b protein
	C>T	Nonsynonymous	28087	A>V	65	ORF8	ORF8b protein
	G>T	Nonsynonymous	25563	Q>H	57	ORF3a	3a Protein
	C>T	Nonsynonymous	28868	P>S	199	N	N

TABLE 2 (Continued)

ID Mexico	Nucleotide change	Synonymous/nonsynonymous	Position genome	Amino acid substitution	Position protein	Gene	Product
	A>G	Nonsynonymous	23403	D>G	614	S	S1
	C>T	Nonsynonymous	1059	T>I	265	ORF1ab	NSP2
	C>T	Synonymous	3037	F	924	ORF1ab	NSP3
	C>T	Nonsynonymous	3768	T>I	1168	ORF1ab	NSP3
	G>T	Synonymous	6421	V	2052	ORF1ab	NSP3
	T>A	Nonsynonymous	6640	H>Q	2125	ORF1ab	NSP3
	C>T	Nonsynonymous	8739	T>I	2825	ORF1ab	NSP4
	C>T	Nonsynonymous	10319	L>F	3352	ORF1ab	3c-like proteinase
	C>T	Synonymous	11575	F	3770	ORF1ab	NSP6
	C>T	Nonsynonymous	14408	P>L	4715	ORF1ab	NSP10
	C>T	Synonymous	17503	F	5746	ORF1ab	Helicase
	A>G	Synonymous	20263	L	6666	ORF1ab	2'-o-ribose methyltransferase
	G>A	Nonsynonymous	21306	R>H	7014	ORF1ab	2'-o-ribose methyltransferase
EPI_ISL_516620	C>T	-	106	-	-	5'-UTR	-
	C>T	-	241	-	-	5'-UTR	-
	G>T	Nonsynonymous	2809	R>S	848	ORF1ab	NSP3
	C>T	Synonymous	3037	F	924	ORF1ab	NSP3
	C>T	Synonymous	5869	Y	1868	ORF1ab	NSP3
	C>T	Nonsynonymous	14408	P>L	4715	ORF1ab	NSP10
	C>T	Synonymous	18829	V	6188	ORF1ab	3'-5' Exonuclease
	A>G	Nonsynonymous	23403	D>G	614	S	S1
	C>T	Nonsynonymous	26042	T>I	217	ORF3a	3a Protein
	G>A	Nonsynonymous	28881	R>K	203	N	N
	G>A	Nonsynonymous	28882	R>K	203	N	N
	G>C	Nonsynonymous	28883	G>R	204	N	N
EPI_ISL_455455	C>T	-	241	-	-	5'-UTR	-
	C>T	Synonymous	3037	F	924	ORF1ab	NSP3
	C>T	Nonsynonymous	14408	P>L	4715	ORF1ab	NSP10
	A>G	Nonsynonymous	23403	D>G	614	S	S1
	C>T	Nonsynonymous	27046	T>M	175	M	M
	G>A	Nonsynonymous	28881	R>K	203	N	N
	G>A	Nonsynonymous	28882	R>K	203	N	N
	G>C	Nonsynonymous	28883	G>R	204	N	N
	G>T	Nonsynonymous	29224	M>I	317	N	N
EPI_ISL_412972	C>T	-	241	-	-	5'-UTR	-
	C>T	Synonymous	3037	F	924	ORF1ab	NSP3
	C>T	Nonsynonymous	14408	P>L	4715	ORF1ab	NSP10
	A>G	Nonsynonymous	23403	D>G	614	S	S1
	G>A	Nonsynonymous	28881	R>K	203	N	N
	G>A	Nonsynonymous	28882	R>K	203	N	N
	G>C	Nonsynonymous	28883	G>R	204	N	N
EPI_ISL_452139	C>T	-	241	-	-	5'-UTR	-
	G>A	Nonsynonymous	28881	R>K	203	N	N
	G>A	Nonsynonymous	28882	R>K	203	N	N
	G>C	Nonsynonymous	28883	G>R	204	N	N
	A>G	Nonsynonymous	23403	D>G	614	S	S1
	C>T	Synonymous	3037	F	924	ORF1ab	NSP3
	C>T	Nonsynonymous	14408	P>L	4715	ORF1ab	NSP10

(Continues)

TABLE 2 (Continued)

ID Mexico	Nucleotide change	Synonymous/nonsynonymous	Position genome	Amino acid substitution	Position protein	Gene	Product
EPI_ISL_424672	C>T	-	241	-	-	5'-UTR	-
	A>G	Nonsynonymous	1308	N>S	348	ORF1ab	NSP2
	C>T	Synonymous	3037	F	924	ORF1ab	NSP3
	C>T	Nonsynonymous	14408	P>L	4715	ORF1ab	NSP10
	C>T	Nonsynonymous	17639	S>L	5792	ORF1ab	Helicase
	A>G	Synonymous	20268	L	6668	ORF1ab	Endornase
	A>G	Nonsynonymous	23403	D>G	614	S	S1
	G>T	Nonsynonymous	27506	G>V	38	ORF7a	7A protein
	C>T	Nonsynonymous	28638	P>L	122	N	N
	A>G	-	29700	-	-	3'-UTR	-
EPI_ISL_516625	C>T	-	241	-	-	5'-UTR	-
	G>T	Nonsynonymous	25996	V>L	202	ORF3a	3a protein
	G>T	Nonsynonymous	29477	D>Y	402	N	N
	A>G	Nonsynonymous	23403	D>G	614	S	S1
	C>T	Synonymous	3037	F	924	ORF1ab	NSP3
	C>T	Synonymous	3992	A	1043	ORF1ab	NSP3
	C>T	Nonsynonymous	6696	P>L	2144	ORF1ab	NSP3
	C>T	Nonsynonymous	7104	T>I	2280	ORF1ab	NSP3
	C>T	Nonsynonymous	14408	P>L	4715	ORF1ab	NSP10
	A>G	Synonymous	20268	L	6668	ORF1ab	Endornase
EPI_ISL_424626	C>T	-	241	-	-	5'-UTR	-
	C>T	Synonymous	2940	L	893	ORF1ab	NSP3
	C>T	Synonymous	3037	F	924	ORF1ab	NSP3
	T>A	Nonsynonymous	6842	S>T	2193	ORF1ab	NSP3
	C>T	Nonsynonymous	14408	P>L	4715	ORF1ab	NSP10
	A>G	Nonsynonymous	23403	D>G	614	S	S1
EPI_ISL_455434	C>T	-	241	-	-	5'-UTR	-
	C>T	Nonsynonymous	1059	T>I	265	ORF1ab	NSP2
	C>T	Synonymous	3037	F	924	ORF1ab	NSP3
	C>T	Nonsynonymous	14408	P>L	4715	ORF1ab	NSP10
	A>C	Nonsynonymous	20756	S>R	6831	ORF1ab	2'-O-Ribose methyltransferase
	A>G	Nonsynonymous	23403	D>G	614	S	S1
	G>T	Nonsynonymous	25563	Q>H	57	ORF3a	3a protein
EPI_ISL_516609	C>T	-	241	-	-	5'-UTR	-
	G>T	Nonsynonymous	25690	G>C	100	ORF3a	3a protein
	C>T	Nonsynonymous	28854	S>L	194	N	N
	A>G	Nonsynonymous	23403	D>G	614	S	S1
	T>C	Synonymous	24076	G	838	S	S2'
	C>T	Synonymous	3037	F	924	ORF1ab	NSP3
	C>T	Synonymous	11074	F	3603	ORF1ab	NSP6
	C>T	Nonsynonymous	14408	P>L	4715	ORF1ab	NSP10
	A>G	Nonsynonymous	16052	K>E	5263	ORF1ab	NSP10
	A>G	Synonymous	20268	L	6668	ORF1ab	Endornase
EPI_ISL_496369	C>T	-	241	-	-	5'-UTR	-
	C>T	Nonsynonymous	28854	S>L	194	N	N
	A>G	Nonsynonymous	23403	D>G	614	S	S1
	C>T	Synonymous	3037	F	924	ORF1ab	NSP3
	A>C	Nonsynonymous	8805	N>T	2847	ORF1ab	NSP4
	C>T	Synonymous	11575	F	3770	ORF1ab	NSP6

TABLE 2 (Continued)

ID Mexico	Nucleotide change	Synonymous/nonsynonymous	Position genome	Amino acid substitution	Position protein	Gene	Product
	C>T	Nonsynonymous	14408	P>L	4715	ORF1ab	NSP10
	C>T	Synonymous	16888	Y	5541	ORF1ab	Helicase
	C>T	Synonymous	19030	H	6255	ORF1ab	3'-5' Exonuclease
	A>G	Synonymous	20268	L	6668	ORF1ab	-
EPI_ISL_493348	C>T	-	241	-	-	5'-UTR	-
	A>G	Nonsynonymous	1558	I>M	431	ORF1ab	NSP2
	C>T	Nonsynonymous	6573	S>F	2103	ORF1ab	NSP3
	C>T	Synonymous	3037	F	924	ORF1ab	NSP3
	C>T	Nonsynonymous	14408	P>L	4715	ORF1ab	Nsp10
	A>G	Synonymous	20268	L	6668	ORF1ab	Endornase
	T>C	Synonymous	22192	I	210	S	S1
	A>G	Nonsynonymous	23403	D>G	614	S	S1
EPI_ISL_493336	C>T	-	241	-	-	5'-UTR	-
	A>G	Nonsynonymous	23403	D>G	614	S	S1
	C>T	Synonymous	3037	F	924	ORF1ab	NSP3
	C>T	Synonymous	4582	N	1439	ORF1ab	NSP3
	C>T	Nonsynonymous	8175	A>V	2637	ORF1ab	NSP3
	C>T	Nonsynonymous	14408	P>L	4715	ORF1ab	NSP10
	A>G	Synonymous	20268	L	6668	ORF1ab	Endornase
EPI_ISL_516611	C>T	-	241	-	-	5'-UTR	-
	C>T	Synonymous	3037	F	924	ORF1ab	NSP3
	G>A	Synonymous	5668	E	1801	ORF1ab	NSP3
	C>T	Synonymous	5884	Y	1873	ORF1ab	NSP3
	C>T	Nonsynonymous	14408	P>L	4715	ORF1ab	NSP10
	A>G	Synonymous	20268	L	6668	ORF1ab	Endornase
	A>G	Nonsynonymous	23403	D>G	614	S	S1
	A>T	Nonsynonymous	23583	Y>F	674	S	S2
	C>T	Nonsynonymous	28854	S>L	194	N	N
EPI_ISL_455438	C>T	-	241	-	-	5'-UTR	-
	C>T	Synonymous	3037	F	924	ORF1ab	NSP3
	A>G	Nonsynonymous	23403	D>G	614	S	S1
	G>A	Synonymous	25183	E	1207	S	S2'
	C>T	Nonsynonymous	14408	P>L	4715	ORF1ab	NSP10
	A>G	Synonymous	20268	L	6668	ORF1ab	Endornase
EPI_ISL_496374	C>T	-	241	-	-	5'-UTR	-
	C>T	Nonsynonymous	28854	S>L	194	N	N
	A>G	Nonsynonymous	23403	D>G	614	S	S1
	C>T	Synonymous	3037	F	924	ORF1ab	NSP3
	C>T	Nonsynonymous	14408	P>L	4715	ORF1ab	NSP10
	A>G	Synonymous	20268	L	6668	ORF1ab	Endornase

Note: Helicase: nsp13_ZBD, nsp13_TB, and nsp_HEL1core. 3'-5' exonuclease: nsp14A2_ExoN and nsp14B_NMT. endoRNase: nsp15-A1 and nsp15B-NendoU. 2'-O-Ribose methyltransferase: nsp16_OMT. 3C-like proteinase: nsp5A.

(InDRE) of the Secretary of Health of Mexico. In addition, the Institute has approved 53 molecular tests from different world companies for the detection of SARS-CoV-2. These tests detect different genes and use different primers with different analytical sensitivity (limit of detection; https://www.gob.mx/cms/uploads/attachment/file/576584/Listado_de_estuches_comerciales_utiles_para_el_diagnostico_de_SARS-CoV-2.pdf).

On the other hand, the governments of Belize and Guatemala obtain diagnostic tests with different primers and with recommendations from the Pan American Health Organization and the World Health Organization (<https://www.pressoffice.gov.bz/government-of-belize-to-procure-covid-19-test-kits-from-cayman-islands/>; <https://www.paho.org/es/documentos/directrices-laboratorio-para-deteccion-diagnostico-infeccion-con-virus-covid-19>). The genomic sequences were aligned

with primers used in the diagnosis of COVID-19 by the RT-PCR using the Sequence Manipulation Site: PCR Products tool v.2 (https://www.bioinformatics.org/sms2/pcr_products.html) and Primer3Plus v.2.4.2 (<https://primer3plus.com/cgi-bin/dev/primer3plus.cgi>), including the sequence NC_045512.2 as reference.

The expect-value (*E* value) is a statistical parameter that describes the probability of the significance of an alignment. The lower the *E*-value, the lower the alignment error; thus, the efficiency of the RT-PCR amplification could show a higher concentration of product per cycle. We evaluated this and other characteristics of these tests,²⁴ such as the variations in specificity reported in the melting curve-based multiplex quantitative RT-PCR (RT-qPCR) Assay for Human Coronaviruses²⁵ and secondary structures for other viruses,²⁶ for this reason, their specificity and *E* values were determined through the basic local alignment search tool (BLAST; https://blast.ncbi.nlm.nih.gov/Blast.cgi?PROGRAM=blastn&PAGE_TYPE=BlastSearch&LINK_LOC=blasthome) and the melting temperature (*T*_m) using Oligo Analyzer program development by Sigma-Aldrich Co. (<http://www.oligoevaluator.com/LoginServlet>).

3 | RESULTS

A total of 187 distinct variants were found in Mexico, 54 in Guatemala, and 39 in Belize. Alignment of genomic sequences of the three countries shared an approximately 99.9% identity. Of these variants, 161 correspond to transitions in Mexico, 50 to transitions in Guatemala and 31 to transitions in Belize (Figure 1) and the rest to transversions. The most common variant in all cases was C>T, which represents an average 52% of the variants that mainly correspond to

ORF1ab (Figure 1). The translation revealed 46 amino acid substitutions and 28 synonyms. The substitutions in the noncoding regions included one in C106T and sixteen in C241T of 5'-UTR, one of 3'-UTR (A29700G), and also, one intergenic variant located between ORF3a and E (T26232C) in Mexico; while in Guatemala, we identified 13 amino acid substitutions and five synonyms.

The variants were distributed in six genes, four of which presented the highest number of mutations (almost 86%). The ORF1ab gene presented the maximum number of mutations, 15 amino acid substitutions, and 16 synonymous, followed by the S gene, with six substitutions and five synonymous. The third gene with the most mutations was the N gene, which contained six nonsynonymous amino acid substitutions and one synonym. And finally, in the ORF8 gene, six substitutions were observed. In the ORF7a gene, only one mutation (G38V) was found; while in the ORF3a gene, one substitution (G196V) and two synonymous (I232) were localized. Figure 1 shows the distribution of mutations in SARS-CoV-2 genomic sequences, including noncoding and intergenic regions. Furthermore, the distribution of the variants in the sequences, where the most common variants in all sequences were C>T and A>G. The variations observed in each genomic sequence are presented in Tables 2–4.

We also localized NSP12 which corresponds to RNA-dependent RNA polymerase (RdRp) and shows that the active sites are formed by the conserved amino acids D760 and D761 (blue spheres). Likewise, there are residues in the 5 Angstrom region (Å) that surround the active aspartates (in magenta bars, amino acids V763, C622, N695, Y619, E811 and F812); and residues H295, C301, C306, C310, H647, C487, C645 and C646 (in orange sticks) correspond to the binding sites of Zn⁺ ions. The mutation P4715L (red spheres) corresponds to amino acid 323 in RdRp and as it can be observed, do not affect, or influence active sites

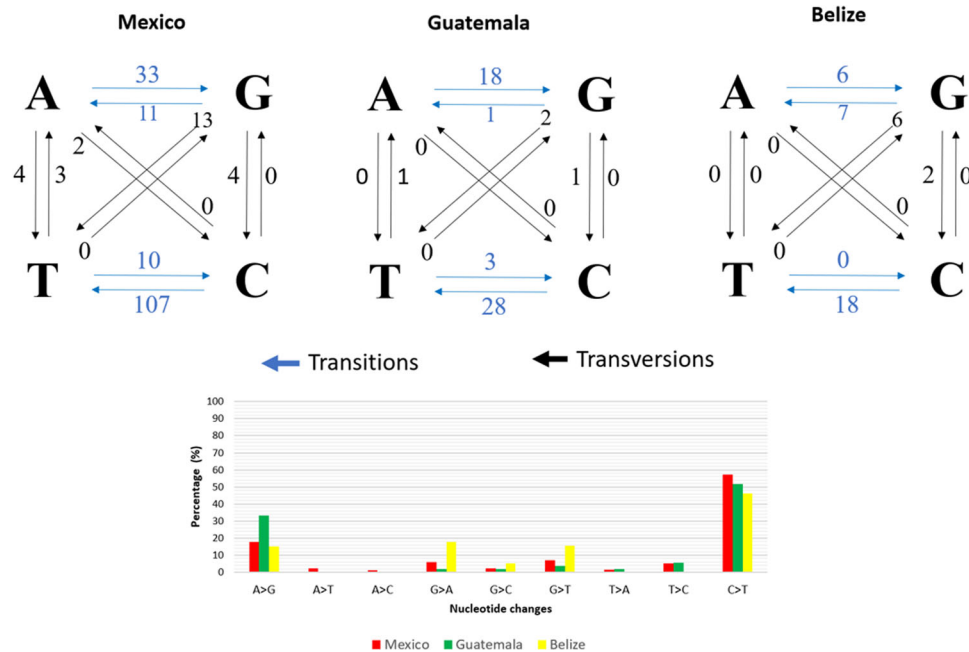


FIGURE 1 Nucleotide variations and distribution identified in the SARS-CoV-2 genomic sequences from Mexico, Guatemala, and Belize

TABLE 3 Nucleotide variants and amino acid substitutions in SARS-CoV-2 genomes in Guatemala

ID Guatemala	Nucleotide change	Synonymous /Nonsynonymous	Position Genome	Amino acid substitution	Position Protein	Gene	Product
EPI_ISL_509710	C>T	----	241	----	----	5'-UTR	----
	C>T	Synonymous	3037	F	924	ORF1ab	NSP2
	A>G	Nonsynonymous	23403	D>G	614	S	S1
	G>T	Nonsynonymous	25563	Q>H	57	ORF3a	3a protein
EPI_ISL_509700	C>T	----	241	----	----	5'-UTR	----
	C>T	Nonsynonymous	14408	P>L	4715	ORF1ab	NSP3
	A>G	Synonymous	20268	L	6668	ORF1ab	NSP3
	A>G	Nonsynonymous	23403	D>G	614	S	S1
EPI_ISL_509699	C>T	----	241	----	----	5'-UTR	----
	C>T	Nonsynonymous	14408	P>L	4715	ORF1ab	
	A>G	Synonymous	20268	L	6668	ORF1ab	
	A>G	Nonsynonymous	23403	D>G	614	S	S1
EPI_ISL_509696	C>T	----	241	----	----	5'-UTR	----
	C>T	Nonsynonymous	14408	P>L	4715	ORF1ab	NSP3
	A>G	Synonymous	20268	L	6668	ORF1ab	NSP3
	A>G	Nonsynonymous	23403	D>G	614	S	S1
EPI_ISL_509695	C>T	----	241	----	----	5'-UTR	----
	C>T	Nonsynonymous	14408	P>L	4715	ORF1ab	NSP3
	A>G	Synonymous	20268	L	6668	ORF1ab	NSP3
	A>G	Nonsynonymous	23403	D>G	614	S	S1
EPI_ISL_509702	C>T	----	241	----	----	5'-UTR	----
	C>T	Synonymous	3037	F	924	ORF1ab	NSP2
	C>T	Nonsynonymous	11379	A>V	3705	ORF1ab	NSP3
	C>T	Nonsynonymous	14408	P>L	4715	ORF1ab	NSP3
	A>G	Synonymous	20268	L	6668	ORF1ab	NSP3
	A>G	Nonsynonymous	23403	D>G	614	S	S1
EPI_ISL_509703	C>T	----	241	----	----	5'-UTR	----
	C>T	Synonymous	3037	F	924	ORF1ab	NSP2
	C>T	Synonymous	14408	L	6668	ORF1ab	NSP3
	A>G	Synonymous	20268	L	6668	ORF1ab	NSP3
	A>G	Nonsynonymous	23403	D>G	614	S	S1
	C>T	Synonymous	25624	S	78	ORF3a	3A PROTEIN
EPI_ISL_509697	C>T	----	241	----	----	5'-UTR	----
	C>T	Synonymous	3037	F	924	ORF1ab	NSP2
	C>T	Synonymous	14408	L	6668	ORF1ab	NSP3
	A>G	Synonymous	20268	L	6668	ORF1ab	NSP3
	A>G	Nonsynonymous	23403	D>G	614	S	S1
EPI_ISL_509698	C>T	----	241	----	----	5'-UTR	----
	C>T	Synonymous	3037	F	924	ORF1ab	nsp2
	C>T	Synonymous	14408	L	6668	ORF1ab	nsp3
	A>G	Synonymous	20268	L	6668	ORF1ab	nsp3
	A>G	Nonsynonymous	23403	D>G	614	S	S1
EPI_ISL_509701	T>A	Nonsynonymous	490	D>E	75	ORF1ab	
	G>A	Nonsynonymous	1590	G>D	442	ORF1ab	NSP1
	C>T	Nonsynonymous	3177	P>L	971	ORF1ab	NSP2
	C>T	Synonymous	8782	S	2839	ORF1ab	NSP3
	T>C	Nonsynonymous	18736	F>L	6157	ORF1ab	NSP3
	G>T	Nonsynonymous	19684	V>L	6473	ORF1ab	NSP3
	C>T	Synonymous	24034	N	824	S	S2'
	T>C	Synonymous	26729	A	207	M	M
	C>T	Nonsynonymous	27635	S>L	81	ORF7a	7a protein
	G>C	Nonsynonymous	28077	V<L	62	ORF8	ORF8b protein
	T>C	Nonsynonymous	28144	L>S	84	ORF8	ORF8b protein
	A>G	Synonymous	29700	----	----	3'-UTR	----

Note: In red: mutations exclusive to Guatemala and in green: mutations that coincide with Mexico.

TABLE 4 Nucleotide variants and amino acid substitutions in SARS-CoV-2 genomes in Belize

ID Guatemala	Nucleotide change	Synonymous /Nonsynonymous	Position Genome	Amino acid substitution	Position Protein	Gene	Product
EPI_ISL_509713	C>T	----	241	----	----	5'-UTR	----
	C>T	Nonsynonymous	1059	T>I	265	ORF1ab	NSP1
	G>A	Nonsynonymous	2808	R>K	848	ORF1ab	NSP2
	C>T	Synonymous	3037	F	924	ORF1ab	NSP2
	G>A	Nonsynonymous	3965	A>T	1234	ORF1ab	NSP2
	C>T	Nonsynonymous	14468	S>L	4735	ORF1ab	NSP3
	G>T	Nonsynonymous	16935	M>I	5557	ORF1ab	NSP3
	G>A	Nonsynonymous	22781	V>I	407	S	S1
	A>G	Nonsynonymous	23403	D>G	614	S	S1
	G>T	Nonsynonymous	25563	Q>H	57	ORF3a	3a protein
A>G	Synonymous	26433	K	63	E	E	
EPI_ISL_509714	C>T	----	241	----	----	5'-UTR	----
	C>T	Nonsynonymous	1059	T>I	265	ORF1ab	NSP1
	C>T	Synonymous	3037	F	924	ORF1ab	NSP2
	C>T	Nonsynonymous	14468	S>L	4735	ORF1ab	NSP3
	C>T	Synonymous	14925	V	4887	ORF1ab	NSP3
	A>G	Nonsynonymous	23403	D>G	614	S	S1
	C>T	Nonsynonymous	23525	H>Y	655	S	S1
	G>T	Nonsynonymous	25563	Q>H	57	ORF3a	3a protein
	A>G	Nonsynonymous	26041	T>A	217	ORF3a	3a protein
	G>T	Synonymous	29179	P	302	N	N
EPI_ISL_509712	C>T	----	241	----	----	5'-UTR	----
	C>T	Synonymous	313	L	48	ORF1ab	NSP1
	C>T	Synonymous	3037	F	924	ORF1ab	NSP2
	C>T	Nonsynonymous	14468	S>L	4735	ORF1ab	NSP3
	A>G	Nonsynonymous	23403	D>G	614	S	S1
	G>T	Nonsynonymous	25456	D>Y	22	ORF3a	3a protein
	G>A	Nonsynonymous	28881	R>K	203	N	N
	G>A	Nonsynonymous	28882	R>K	203	N	N
EPI_ISL_509711	C>T	----	241	----	----	5'-UTR	----
	C>T	Synonymous	313	L	48	ORF1ab	nsp1
	C>T	Synonymous	3037	F	924	ORF1ab	NSP2
	C>T	Nonsynonymous	14468	S>L	4735	ORF1ab	NSP3
	A>G	Nonsynonymous	23403	D>G	614	S	S1
	G>T	Nonsynonymous	25456	D>Y	22	ORF3a	3a protein
	G>A	Nonsynonymous	28881	R>K	203	N	N
	G>A	Nonsynonymous	28882	R>K	203	N	N
G>C	Nonsynonymous	28883	G>R	204	N	N	

Note: In red: mutations exclusive to BELIZE and in green: mutations that coincide with MEXICO.

(Figure 2A). Also, Figure 2B shows an overall view of the trimeric spike protein. The D614G mutations found in Mexico, Belize and Guatemala were 29 out of a total of 37 strains.

In Mexico, the genome sequences that we found had four sequences with lineage A5 and clade S; four sequences with lineage A1 and clade S; three sequences with lineage B1 and clade G; six sequences with lineage B1.5 with clade G; one sequence with lineage B1 and clade GH; two sequences with lineage B1.1 and clade GR; one sequence with lineage B1.2 and clade GH; one sequence with lineage B1 and clade GR and one sequence with lineage B1.75 with clade G. However, in Guatemala, we found four genome sequences with lineage B1.5 with clades O, four genome sequences with lineage B1.5 and clades G, one genome sequence with lineage B1 and clade H, and another with lineage A3 with clade S. In the genome sequences from Belize, we found

two B1 lineages with H clades, and two other genomes with the B1.1 lineage and R clade.

A 3D model of ORF8 protein was obtained using the data of that proposed by Yang Zhang Lab, with its binding sites. ORF8 protein is 121 residues in length.²² Figure 3 illustrates the spatial distribution of the L84S mutation along with R48, G50, L57, P56, Q72, and Y73 residues, which could be a glycerol binding site. S97 and L98 could be a region that binds to an Hg⁺ ion likewise, ORF8 could be related to pathogenesis.^{14,27}

The in silico analysis of the primers is used in the RT-qPCR for detection of SARS-CoV-2 (Table 5). The results reported by Yan et al.²⁸ and Udugama et al.,²⁹ show that most of the primers contain 23%–58% of guanine-cytosine content (GC). These generate a few dimers, as well as having a very weak or weak secondary structure, and possess a melting temperature (Tm) among 48.7°C–71.7°C. Also,

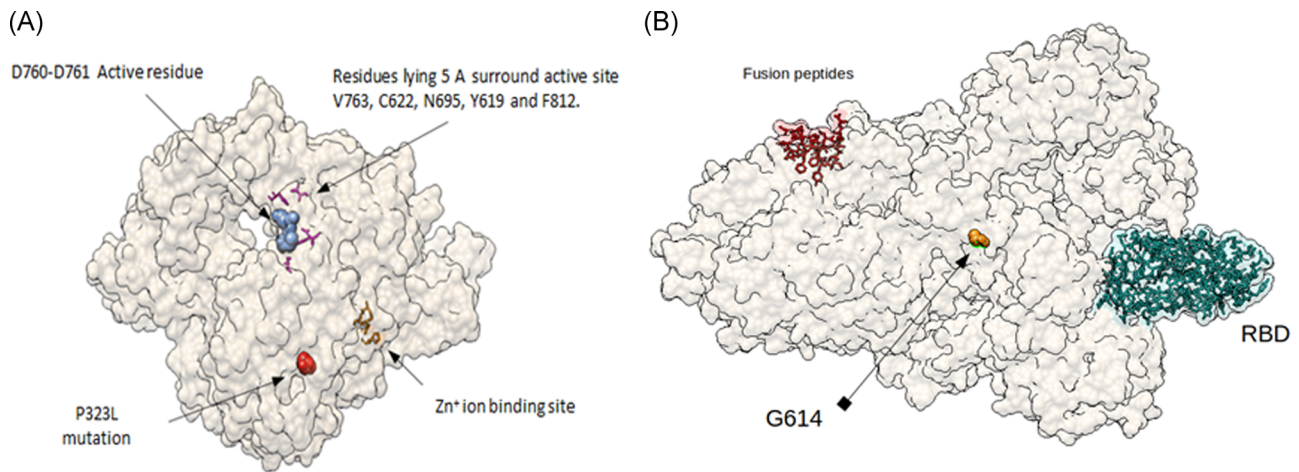


FIGURE 2 Mutations P4715L and G614G: (A) amino acid P4715 in red spheres, correspondent to residue 323 in RdRp protein of SARS-CoV-2. In blue spheres D760 and D761 active sites. In magenta sticks, V763, C622, N695, Y619, and F812 residues. These residues, lying 5 Å surrounding DD active site. In orange sticks, H295, C301, C306, and C310 residues (Zn⁺ ion binding site). Structure was downloaded from PDB (<https://www.rcsb.org/>) ID 6M71.pdb, and edited using UCSF Chimera, v.1.12. (B) Amino acid substitution D614G on spike (original model downloaded from [rcsb.org](https://www.rcsb.org/), code 6VSB.pdb). G614 mutation is far away from important residues for attachment (RBD in green light spheres) and fusion (fusion peptides, red spheres, residues 788–806) with membrane. Visualization using Chimera UCSF, v.1.12

we show the high sensitivity of the primers used because the *E* value is close to zero, except in the set designed by CDC from the United States where the *E* value is positive, indicating low sensitivity.

Primers designed by the Chinese Center for Disease Control and Prevention (China CDC), Charité (Germany), and the National Institute of Infectious Diseases (Japan) for the RdRp, N and S genes give a product using Primer3Plus, and similarly, multiple alignments (Table 5). This indicates a high sensitivity to these primers, however, four sets of primers used by the Centers for Disease Control and Prevention (CDC US) present low sensitivity to RdRp, S, and N

amplicons. They are misaligned with the primer forward that can recognize 11/19 base pairs causing low sensitivity.

4 | DISCUSSION

The genomic sequences of first SARS-CoV-2 strain in Mexico (hCoV/Mexico/CDMX/InDRE_01/2020) show high identity with the sequence reported in China Wuhan-Hu-1 (NC_045512.2), it only differs in seven nucleotide substitutions.⁸ This high sequence identity

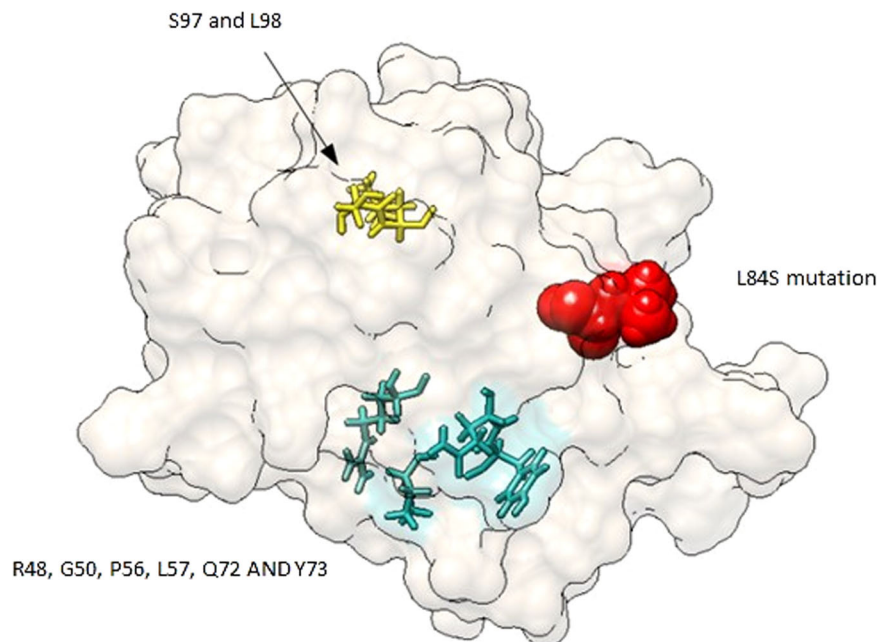


FIGURE 3 Spatial distribution of the mutation L84S in the ORF8 protein. L84P mutation is represented in red sticks and in wire light sea green color, R48, G50, L57, P56, Q72, and Y73. In yellow sticks, a probable Hg⁺ ion binding site

TABLE 5 In silico analysis of primers used for diagnosis of COVID-19

Institution	Gene	Primers (5'-3')	Estimated length (bp)	Position	Percentage of identities ^a (%)	Evalue ^a	Tm ^b (°C)	GC (%)	Secondary structure ^b	Dimers ^b
Center for Disease Control and Prevention of the United States, CDC US ³⁰	N	GACCCCAAAATCAGCGAAAT	72	28287-28358	100	3e-07	64.9	45	None	No
		TCTGGTTACTGCCAGTTGAATCTG	67	29164-29230	100	2e-09	66.2	45.8	Strong	No
		TFACAAACATTGGCCGCAAA								
		GCGGACATTCGGAAGAA								
		GGGAGCCTTGAATACACCAAAA								
		TGTAGCACGATTGCAGCATTG								
AGATTTGGACCTGGAGCG										
RdRp	GAGCGGTGTCACCAAGT	160*	14413-14572	52	3.6	67.7	57.9	None	No	
		65	66.9	60	Weak	No				
Chinese Center for Disease Control and Prevention, China CDC ³¹	ORF1ab	CCCTGTGGGTTTTACACTTAA	119	13342-13460	100	7e-08	60.3	42.9	Moderate	Yes
		ACGATTGTGCATCAGCTGA	100	1e-06	63.3	47.4	Very weak	No		
		GGGAACTTCTCCTGCTAGAAT	99**	28881-28979	86	2e-08	63.6	50	Weak	No
Charité, Germany ²⁹	RdRp	CAGACATTTGCTCTCAAGCTG	100	2e-08	63.9	45.5	Weak	No		
		GTGARATGTCATGTGTGGCGG	100*	15431-15530	100	1e-07	63.7	54.5	Very weak	No
Hong Kong University ²²	ORF1b-nsp14	CARATGTTAAASACACTATTAGCATA	113	26269-26381	100	1e-10	59.2	34.6	Weak	No
		ACAGGTACGTTAATAGTTAATAGCGT	100	2e-08	65.4	45.5	Weak	No		
		ATATTGCAGCAGTACGCACACA	100	18778-18909	100	2e-05	65.7	45.0	None	No
National Institute of Infectious Diseases, Japan ³³	ORF1a	TGGGGYTTTACRGGTAACT	132	29125-29282	100	3e-07	63.7	45	Weak	No
		AACRCGCTTAAACAAAGCACTC	95	7e-05	64.0	55.0	None	No		
		TAATCAGACAAGGAACTGATTA	110	29145-29254	100	2e-08	55.5	31.8	Moderate	No
National Institute of Health, Thailand ³⁴	N	CGAAGGTGTGACTTCCATG	158*	29125-29282	100	1e-06	61.8	52.8	Moderate	Yes
		AAATTTGGGGACCAGGAAC	100	3e-07	63.7	45	Weak	No		
		TGGCAGCTGTAGGTCAAC	95	7e-05	64.0	55.0	None	No		
		TTCGGATGCTCGAACTGCACC	413	484-896	100	7e-08	71.7	57.1	Moderate	No
		CTTTACCAGCACGTGCTAGAAGG	346	492-837	100	6e-09	65.8	52.2	Weak	No
		CTCGAACTGCACCTCATGG	100	1e-06	64.7	57.9	None	No		
National Institute of Health, Thailand ³⁴	S	CAGAAATTTGTTATCGACATAGC	547	24354-24900	100	2e-08	58.0	40.9	Very weak	No
		TTGGCAAAATTCAAAGACTCACTT	547	24354-24900	100	2e-09	64.6	33.3	Very weak	No
		TGTGGTTTCATAAAAAATTCCTTTGTG	494*	24363-24856	100	4e-10	64.5	32	None	No
		CTCAAGACTCACTTCTCCAC	95	8e-08	59.6	45.5	Weak	No		
National Institute of Health, Thailand ³⁴	N	ATTTGAAAAAAGACACCTTCAC	100	6e-09	60.9	34.8	Weak	No		
		CGTTTGGTGGACCCTCAGAT	57	28320-28376	100	3e-07	66.2	55.0	None	No
		CCCCACTGCTTCTCCATT	100	1e-06	67.3	57.9	None	No		

Note: Forward and reverse.

^aCalculated by BLAST.^bCalculated by Oligo Evaluator (Sigma-Aldrich Co.).

**Estimated by alignment using Clustal Omega.

**No product in the EPI_ISL_412972 sequence.

has been attributed to the recent spread of the virus in humans, suggesting a common lineage and source.^{10,35} Our results show 84% more transitions than transversions. The effects of transition and transversion mutations have been studied in influenza (H1N1) and the human immunodeficiency virus virus, these studies conclude that it is likely that transversions cause radical changes in amino acids^{29,36} that could be involved in the high genomic conservation of the new coronavirus.

Different reports of variant analysis of SARS-CoV-2 genomes show similar results to those of Mexico, Belize, and Guatemala, for example, Koyama et al.³⁷ reported that C>T was the most common variant; they also identified mutations in C3037T (F924), C14408T (P4715L) in RdRp, ORF1ab and, A23403G (D614G) in the spike, this was reported mainly in Europe and the United States.^{35,38} Additionally, D614G formed the largest phylogenetic clade including C241T, F924, and P4715L, while the second largest clade was T28144C (L84S) present in ORF8, which was reported days after the outbreak in travelers from Wuhan. Among the L84S clade, the L84S/C17747T (P5828L) subclade was more frequent in the United States.^{37,38} Regarding the P4715L mutation, it corresponds to amino acid residue 323 in the RdRp; however, it does not affect or influence the active sites (Figure 2A), according to Yang et al.,³⁹ who predicted active site residues in the same region. Similarly, Khailany et al.,⁴⁰ reported that C>T was the most frequent mutation observed and also found C8782T (S2839) mutations in ORF1ab and T28144C (L84S) in ORF8 genes. We did not identify the mutation in the C29095T (F274) N gene.³⁹

Moreover, current evidence of the mutation of an aspartate (D) at position 614 to glycine (G) in spike is possibly related to increased infectivity,⁴¹ but also gives a more pathogenic strain. The G614G mutation alters the fusion of the cell membrane and the data reveals that it is located in a highly glycosylated region that also allows the identification of two viral clades.^{39,42} The aspartate strain has been found in cases reported on the West Coast of United States, while the glycine strain has been reported on the East Coast.⁴³ In Mexico, our study revealed the presence of the D614 in samples, identified in a smaller number of cases at the moment of sequencing.

SARS-CoV-2 genomes have two major lineages with sublineages A (1, 2, 3, and 5) and B (1, 1.1, 2, 3, and 4).⁴⁴ In Mexico, Taboada et al.⁴⁵ found that the lineages changed from late February to March from A2 to B1. Considering that we selected only the complete sequences, we found a higher proportion of B lineages and clades G as in Guatemala and Belize.

Lineages have been associated with certain clinical manifestations.³⁵ Lineage A has sequences from Europe and conforms to a human coronavirus (HCoV-OC43 and HCoV-HKU1), may be associated with self-limiting upper respiratory infections, and occasionally, with lower respiratory tract infections; while lineage B may cause severe lower respiratory tract infections with acute respiratory distress syndrome and extrapulmonary manifestations.⁴³

We found a mutation in the noncoding regions 5'-UTR (C241T), this type of mutation in UTRs of SARS-Cov-2 has been studied recently, suggesting that C241T in 5'-UTR appeared early during the

outbreak, and could be key in virus replication and RNA folding,⁴⁶ affecting the stem-loop 5b (SL5b)^{47,48} and the host defense.⁴⁹ The intergenic mutation A29700G located between ORF3a and E genes might emerge through adenosine deaminase acting on RNA (ADAR) and could be important in the antiviral response^{28,35,50} reducing the stability in the RNA fold.²⁹

Activation of the SARS-CoV-2 spike protein via sequential proteolytic cleavage can be at two distinct sites. For many CoVs, the spike protein is cleaved at the boundary between the S1 and S2 subunits (residues 685 and 686), which remain non covalently bound in the prefusion conformation while for all CoVs, the spike is further cleaved by host proteases at the so-called S2 site located immediately upstream of the fusion peptide (residues 788–806).⁵¹ Also, RBD is constituted by residues 333–527 and belongs to a region that attaches to hACE2, a highly conserved cryptic epitope in the receptor-binding domains of SARS-CoV-2 and SARS-CoV.⁵² As we can see, the D614G mutation is not between important regions known, but recently has been associated with high prevalence, from <1% in January to 69% in March. The global spread of SARS-CoV-2 subtype with spike protein D614G mutation is shaped by Human Genomic Variations that regulate the expression of TMPRSS2 and MX1 genes, although the mechanism by which such a phenomenon occurs is not clear yet.⁵³

The ORF8 protein has 121 residues in length and very little is known about its function. Nevertheless, Zhang et al.²² have proposed a 3D model along with its binding sites. The L84S mutation in genomic sequences in Mexico can indicate that the circulating strain shows a different characteristic, like the Wuhan strain. However, the number of analyzed samples is a limitation of guarantee. Due to several reports of low sensitivity in the RT-PCR test, which is not considered the gold standard for diagnosis of COVID-19,^{54,55} we analyzed a predictive evaluation of the sensitivity of the primers used (Table 5).

The N gene has a high degree of conservation in coronaviruses,⁵⁶ however, in our study, the N gene is the third with the highest number of mutations, following the ORF1ab and S genes. The results suggest a high sensitivity of the primers. Nevertheless, that designed by CDC (US) for the RdRp gene, could generate low sensitivity of the forward and reverse primer related to the few complementary bases already reported.⁵⁷ Besides this, the mutations AAC (28881–28883) in the N gene could decrease sensitivity because they are part of the region where the primer is attached to the template strand. As a consequence, it is not recognized by Primer3Plus. We considered that not all primers possess high sensitivity for diagnosing of COVID-19, and the mutations in the genomic sequences may decrease just the sensitivity. Recently in China, it has been reported that non-specific primers may amplify high concentrations of human cathepsin C (CTSC) and messenger RNA in the tonsils. This could cause interference in diagnosing COVID-19,⁵⁸ which could explain why RT-PCR should not be considered the gold standard. Furthermore, the test presents other problems, such as those related to errors in swab tests, causing improper extraction of viral RNA.⁵⁹ A comprehensive review of the diagnosis of COVID-19 can be found at Yan et al.²² and Li and Ren.⁶⁰

As time passes, mutations in the genomic sequences of SARS-CoV-2 could appear in the highly conserved regions and the effectiveness of the diagnostic methods could be compromised. Factors, such as correct sampling, conservation and transport of the sample, extraction⁶¹ quality and integrity of RNA,³⁷ calibration of the thermocycler, and optimal amplification conditions, may influence the results. Likewise, the design of primers in conserved regions is essential, and experimental studies are required for a wider understanding. Finally, several questions related to the mutations remain, a very important one is whether these mutations are related to the observed case-fatality rate. Until September 13, 2020, Mexico has a very high case-fatality rate of 10.6%, Belize 1.3%, and Guatemala 3.6%, in addition to a high number of people with comorbidities.⁶²

ACKNOWLEDGEMENTS

The authors acknowledge all the people and laboratories responsible for the sequencing and submitting to the GISAID and NCBI databases for public consultation. Without them, this study could not have been carried out, likewise, we declare that the rights to the sequences belong to the people who participated in it, we have not participated in this. Additionally, we recognize the efforts of all the personnel involved in care of patients with COVID-19. Also, the authors thank Charlotte Grundy for her assistance and the National Technology of Mexico (TecNM) project 8703.20-P.

CONFLICT OF INTEREST

The authors declare that we have no conflicts of interest.

CONTRIBUTION STATEMENT

Formal analysis, investigation, methodology, data curation, software, writing: original draft, writing: review and editing: María T. Hernández-Huerta and Laura P.-C. Mayoral. *Formal analysis, investigation and software:* Carlos R. Díaz. *Formal analysis, investigation and funding acquisition:* Margarito Martínez Cruz. *Formal analysis and investigation:* Gabriel Mayoral-Andrade. *Resources and investigation:* Luis M. S. Navarro. *Investigation:* María D. S. Pina Canseco, Ruth M. Cruz, Eduardo P.-C. Mayoral, and Gabriela V. Martínez. *Writing: review and editing:* Eli C. Parada. *Funding acquisition and investigation:* Alma D. P. Santiago. *Conceptualization, supervision, visualization, project administration, writing: review and editing:* Eduardo Pérez-Campos and Carlos A. Matias-Cervantes.

DATA AVAILABILITY STATEMENT

The data that support the findings of this study are available from the corresponding author upon reasonable request.

ORCID

María Teresa Hernández-Huerta  <https://orcid.org/0000-0003-2182-2540>

Laura Pérez-Campos Mayoral  <https://orcid.org/0000-0003-4140-4661>

Carlos Romero Díaz  <https://orcid.org/0000-0002-7524-067X>

Margarito Martínez Cruz  <https://orcid.org/0000-0002-0379-4630>

Gabriel Mayoral-Andrade  <https://orcid.org/0000-0002-2957-8565>

Luis Manuel Sánchez Navarro  <https://orcid.org/0000-0003-4161-751X>

María Del Socorro Pina-Canseco  <https://orcid.org/0000-0002-9486-5093>

Ruth Martínez Cruz  <https://orcid.org/0000-0002-6472-8709>

Eduardo Pérez-Campos Mayoral  <https://orcid.org/0000-0002-6032-7609>

Alma Dolores Pérez Santiago  <https://orcid.org/0000-0002-4410-7307>

Gabriela Vásquez Martínez  <https://orcid.org/0000-0003-3239-3737>

Eduardo Pérez-Campos  <https://orcid.org/0000-0001-6720-7952>

Carlos Alberto Matias-Cervantes  <https://orcid.org/0000-0002-3476-1743>

REFERENCES

1. Wu F, Zhao S, Yu B, et al. A new coronavirus associated with human respiratory disease in China. *Nature*. 2020;579(7798):265–269. <https://doi.org/10.1038/s41586-020-2008-3>
2. Chan JFW, Yuan S, Kok KH, et al. A familial cluster of pneumonia associated with the 2019 novel coronavirus indicating person-to-person transmission: a study of a family cluster. *Lancet*. 2020;395(10223):514–523. [https://doi.org/10.1016/S0140-6736\(20\)30154-9](https://doi.org/10.1016/S0140-6736(20)30154-9)
3. Zhu N, Zhang D, Wang W, et al. A novel coronavirus from patients with pneumonia in China, 2019. *N Engl J Med*. 2020;382(8):727–733. <https://doi.org/10.1056/NEJMoa2001017>
4. Elbe S, Buckland-Merrett G. Data, disease and diplomacy: GISAID's innovative contribution to global health. *Glob Chall*. 2017;1(1):33–46. <https://doi.org/10.1002/gch2.1018>
5. Institute for Health Metrics and Evaluation. COVID-19 projections. University of Washington. 2020. <https://covid19.healthdata.org/global?view=total-deaths&tab=trend>
6. Eybpoosh S, Haghdoost AA, Bahrampour A, Azadmanesh K, Zolala F. Molecular epidemiology of infectious diseases. *Electron Physician*. 2017;9(8):5149–5158. <https://doi.org/10.19082/5149>
7. Ornelas-Aguirre JM. El nuevo coronavirus que llegó de Oriente: análisis de la epidemia inicial en México [The new coronavirus that came from the East: analysis of the initial epidemic in Mexico]. *Gac Med Mex*. 2020;156:209–217. <https://doi.org/10.24875/GMM.20000165>
8. Garcés-Ayala F, Araiza-Rodríguez A, Mendieta-Condado E, et al. Full genome sequence of the first SARS-CoV-2 detected in Mexico. *Arch Virol*. 2020;165(9):2095–2098. <https://doi.org/10.1007/s00705-020-04695-3>
9. Lu R, Zhao X, Li J, et al. Genomic characterisation and epidemiology of 2019 novel coronavirus: implications for virus origins and receptor binding. *Lancet*. 2020;395(10224):565–574. [https://doi.org/10.1016/S0140-6736\(20\)30251-8](https://doi.org/10.1016/S0140-6736(20)30251-8)
10. Cui J, Li F, Shi ZL. Origin and evolution of pathogenic coronaviruses. *Nat Rev Microbiol*. 2019;17(3):181–192. <https://doi.org/10.1038/s41579-018-0118-9>
11. Chan JFW, Kok KH, Zhu Z, et al. Genomic characterization of the 2019 novel human-pathogenic coronavirus isolated from a patient with atypical pneumonia after visiting Wuhan. *Emerg Microbes Infect*. 2020;9(1):221–236. <https://doi.org/10.1080/22221751.2020.1719902>
12. Liu DX, Fung TS, Chong KK, Shukla A, Hilgenfeld R. Accessory proteins of SARS-CoV and other coronaviruses. *Antiviral Res*. 2014;109:97–109. <https://doi.org/10.1016/j.antiviral.2014.06.013>
13. Baranov PV, Henderson CM, Anderson CB, Gesteland RF, Atkins JF, Howard MT. Programmed ribosomal frameshifting in decoding the

- SARS-CoV genome. *Virology*. 2005;332(2):498–510. <https://doi.org/10.1016/j.virol.2004.11.038>
14. Huang X, Pearce R, Zhang Y. De novo design of protein peptides to block association of the SARS-CoV-2 spike protein with human ACE2. *Aging*. 2020;12(12):11263–11276. <https://doi.org/10.18632/aging.103416>
 15. He Y, Zhou Y, Liu S, et al. Receptor-binding domain of SARS-CoV spike protein induces highly potent neutralizing antibodies: implication for developing subunit vaccine. *Biochem Biophys Res Commun*. 2004;324(2):773–781. <https://doi.org/10.1016/j.bbrc.2004.09.106>
 16. Lokman SM, Rasheduzzaman M, Salaudinn A, et al. Exploring the genomic and proteomic variations of SARS-CoV-2 spike glycoprotein: a computational biology approach. *Infect Genet Evol*. 2020;84:104389. <https://doi.org/10.1016/j.meegid.2020.104389>
 17. Issa E, Merhi G, Panossian B, Salloum T, Tokajian S. SARS-CoV-2 and ORF3a: nonsynonymous mutations, functional domains, and viral pathogenesis. *mSystems*. 2020;5(3):e00266–20. <https://doi.org/10.1128/mSystems.00266-20>
 18. Hassan SS, Choudhury PP, Basu P, Jana SS. Molecular conservation and differential mutation on ORF3a gene in Indian SARS-CoV2 genomes. *Genomics*. 2020;112(5):3226–3237. <https://doi.org/10.1016/j.ygeno.2020.06.016>
 19. Yang Zhang Research Group. Zhang Lab. University of Michigan. <https://zhanglab.ccmb.med.umich.edu/COVID-19/>
 20. Wrapp D, Wang N, Corbett KS, et al. Cryo-EM structure of the 2019-nCoV spike in the prefusion conformation. *Science*. 2020;367(6483):1260–1263. <https://doi.org/10.1126/science.abb2507>
 21. Gao Y, Yan L, Huang Y, et al. SARS-Cov-2 RNA-dependent RNA polymerase in complex with cofactors. RCSB PDB. EMDDataResource: EMD-30127. 2020. <https://doi.org/10.2210/pdb6M71/pdb>
 22. Yang Zhang Research Group. Zhang Lab. University of Michigan. <https://zhanglab.ccmb.med.umich.edu/>
 23. Corman VM, Landt O, Kaiser M, et al. Detection of 2019 novel coronavirus (2019-nCoV) by real-time RT-PCR. *Euro Surveill*. 2020;25(3):2000045. <https://doi.org/10.2807/1560-7917.ES.2020.25.3.2000045>
 24. Houg HSH, Norwood D, Ludwig GV, Sun W, Lin M, Vaughn DW. Development and evaluation of an efficient 3'-noncoding region based SARS coronavirus (SARS-CoV) RT-PCR assay for detection of SARS-CoV infections. *J Virol Methods*. 2004;120(1):33–40. <https://doi.org/10.1016/j.jviromet.2004.04.008>
 25. Wan Z, Zhang Y, He Z, et al. A melting curve-based multiplex RT-qPCR assay for simultaneous detection of four human coronaviruses. *Int J Mol Sci*. 2016;17(11):1880. <https://doi.org/10.3390/ijms17111880>
 26. Chou KX, Williams-Hill DM. Improved TaqMan real-time assays for detecting hepatitis A virus. *J Virol Methods*. 2018;254:46–50. <https://doi.org/10.1016/j.jviromet.2018.01.014>
 27. Chen S, Zheng X, Zhu J, et al. Extended ORF8 gene region is valuable in the epidemiological investigation of severe acute respiratory syndrome-similar coronavirus. *J Infect Dis*. 2020;222(2):223–233. <https://doi.org/10.1093/infdis/jiaa278>
 28. Yan Y, Chang L, Wang L. Laboratory testing of SARS-CoV, MERS-CoV, and SARS-CoV-2 (2019-nCoV): current status, challenges, and countermeasures. *Rev Med Virol*. 2020;30(3):e2106. <https://doi.org/10.1002/rmv.2106>
 29. Udagama B, Kadhiresan P, Kozlowski HN, et al. Diagnosing COVID-19: the disease and tools for detection. *ACS Nano*. 2020;14(4):3822–3835. <https://doi.org/10.1021/acsnano.0c02624>
 30. U.S. CDC. CDC 2019-Novel coronavirus (2019-nCoV) real-time RT-PCR diagnostic panel. Division of Viral Diseases, U.S. Centers for Disease Control and Prevention, Atlanta. 2020.
 31. China CDC. Specific primers and probes for detection 2019 novel coronavirus. China National Institute For Viral Disease Control and Prevention, Beijing. 2020.
 32. Hong Kong University. Detection of 2019 novel coronavirus (2019-nCoV) in suspected human cases by RT-PCR. School of Public Health. Hong Kong University, Hong Kong. 2020.
 33. Naganori N, Shirato K, Katano H, et al. Detection of second case of 2019-nCoV infection in Japan. Department of Virology III, National Institute of Infectious Diseases, Japan. 2020.
 34. National Institute of Health. Diagnostic detection of novel coronavirus 2019 by real time RT-PCR. Department of Medical Sciences, Ministry of Public Health, Thailand. 2020.
 35. Gralinski LE, Menachery VD. Return of the coronavirus: 2019-nCoV. *Viruses*. 2020;12(2):135. <https://doi.org/10.3390/v12020135>
 36. Lyons DM, Luring AS. Evidence for the selective basis of transition-to-transversion substitution bias in two RNA viruses. *Mol Biol Evol*. 2017;34(12):3205–3215. <https://doi.org/10.1093/molbev/msx251>
 37. Koyama T, Platt D, Parida L. Variant analysis of COVID-19 genomes. *Bull World Health Organ*. 2020;98(7):495–504. <https://doi.org/10.2471/BLT.20.253591>
 38. Mishra A, Pandey AK, Gupta P, et al. Mutation landscape of SARS-CoV-2 reveals three mutually exclusive clusters of leading and trailing single nucleotide substitutions. *bioRxiv*. 2020;2020:1–18. <https://doi.org/10.1101/2020.05.07.082768>
 39. Yang J, Roy A, Zhang Y. Protein-ligand binding site recognition using complementary binding-specific substructure comparison and sequence profile alignment. *Bioinformatics*. 2013;29(20):2588–2595. <https://doi.org/10.1093/bioinformatics/btt447>
 40. Khailany RA, Safdar M, Ozaslan M. Genomic characterization of a novel SARS-CoV-2. *Gene Rep*. 2020;19:100682. <https://doi.org/10.1016/j.genrep.2020.100682>
 41. Grubaugh ND, Hanage WP, Rasmussen AL. Making sense of mutation: what D614G means for the COVID-19 pandemic remains unclear. *Cell*. 2020;182(4):794–795. <https://doi.org/10.1016/j.cell.2020.06.040>
 42. Becerra-Flores M, Cardozo T. SARS-CoV-2 viral spike G614 mutation exhibits higher case fatality rate. *Int J Clin Pract*. 2020;74:e13525. <https://doi.org/10.1111/ijcp.13525>
 43. Brufsky A. Distinct viral clades of SARS-CoV-2: implications for modeling of viral spread. *J Med Virol*. 2020;92:1386–1390. <https://doi.org/10.1002/jmv.25902>
 44. Rambaut A, Holmes EC, O'Toole Á, et al. A dynamic nomenclature proposal for SARS-CoV-2 lineages to assist genomic epidemiology. *Nat Microbiol*. 2020;5(11):1403–1407. <https://doi.org/10.1038/s41564-020-0770-5>
 45. Taboada B, Vazquez-Perez JA, Muñoz-Medina JE, et al. Genomic analysis of early SARS-CoV-2 variants introduced in Mexico. *J Virol*. 2020;94(18):e01056–20. <https://doi.org/10.1128/JVI.01056-20>
 46. Rangan R, Zheludev IN, Hagey RJ, et al. RNA genome conservation and secondary structure in SARS-CoV-2 and SARS-related viruses: a first look. *RNA*. 2020;26(8):937–959. <https://doi.org/10.1261/rna.076141.120>
 47. Zhang C, Zheng W, Huang X, Bell EW, Zhou X, Zhang Y. Protein structure and sequence reanalysis of 2019-nCoV genome refutes snakes as its intermediate host and the unique similarity between its spike protein insertions and HIV-1. *J Proteome Res*. 2020;19(4):1351–1360. <https://doi.org/10.1021/acs.jproteome.0c00129>
 48. Andrews RJ, Peterson JM, Haniff HS, et al. An in silico map of the SARS-CoV-2 RNA structurome. *bioRxiv*. 2020;2020:1–18. <https://doi.org/10.1101/2020.04.17.045161>
 49. Ryder SP. Analysis of rapidly emerging variants in structured regions of the SARS-CoV-2 genome. *bioRxiv*. 2020;2020:1–40. <https://doi.org/10.1101/2020.05.27.120105>
 50. Tomaselli S, Galeano F, Locatelli F, Gallo A. ADARs and the balance game between virus infection and innate immune cell response. *Curr Issues Mol Biol*. 2015;17:37–51.

51. Dramé M, Tabue Teguo M, Proye E, et al. Should RT-PCR be considered a gold standard in the diagnosis of COVID-19? *J Med Virol.* 2020;92:2312–2313. <https://doi.org/10.1002/jmv.25996>
52. Yuan M, Wu NC, Zhu X, et al. A highly conserved cryptic epitope in the receptor binding domains of SARS-CoV-2 and SARS-CoV. *Science.* 2020;368(6491):630–633. <https://doi.org/10.1126/science.abb7269>
53. Bhattacharyya C, Das C, Ghosh A, Singh AK, et al. Global spread of SARS-CoV-2 subtype with spike protein mutation D614G is shaped by human genomic variations that regulate expression of TMPRSS2 and MX1 genes. *bioRxiv.* 2020;2020:1–30. <https://doi.org/10.1101/2020.05.04.075911>
54. Belouzard S, Chu VC, Whittaker GR. Activation of the SARS coronavirus spike protein via sequential proteolytic cleavage at two distinct sites. *Proc Natl Acad Sci USA.* 2009;106(14):5871–5876. <https://doi.org/10.1073/pnas.0809524106>
55. Hernández-Huerta MT, Pérez-Campos Mayoral L, Sánchez Navarro LM, et al. Should RT-PCR be considered a gold standard in the diagnosis of COVID-19? *J Med Virol.* 2020;2020:26228. <https://doi.org/10.1002/jmv.26228>
56. Johns Hopkins Center for Health Security. Fact sheet: comparison of national RT-PCR primers, probes, and protocols for SARS-CoV-2 diagnostics. <https://www.centerforhealthsecurity.org/resources/COVID-19/COVID-19-fact-sheets/200410-RT-PCR.pdf>
57. Vogels CBF, Brito AF, Wyllie AL, et al. Analytical sensitivity and efficiency comparisons of SARS-CoV-2 RT-qPCR primer–probe sets. *Nat Microbiol.* 2020;5:1299–1305. <https://doi.org/10.1038/s41564-020-0761-6>
58. Liu W. Non-specific primers reveal false-negative risk in detection of COVID-19 infections. *medRxiv.* 2020;2020:1–13. <https://doi.org/10.1101/2020.04.07.20056804>
59. Xie X, Zhong Z, Zhao W, Zheng C, Wang F, Liu J. Chest CT for typical coronavirus disease 2019 (COVID-19) pneumonia: relationship to negative RT-PCR testing. *Radiology.* 2020;296(2):E41–E45. <https://doi.org/10.1148/radiol.2020200343>
60. Li C, Ren L. Recent progress on the diagnosis of 2019 novel coronavirus. *Transbound Emerg Dis.* 2020;67(4):1485–1491. <https://doi.org/10.1111/tbed.13620>
61. Grant PR, Turner MA, Shin GY, Nastouli E, Levett LJ. Extraction-free COVID-19 (SARS-CoV-2) diagnosis by RTPCR PCR to increase capacity for national testing programme during a pandemic. *BioRxiv.* 2020;2020:1–6. <https://doi.org/10.1101/2020.04.06.028316>
62. Johns Hopkins University. Mortality analyses, maps & trends. 2020. <https://coronavirus.jhu.edu/data/mortality>

How to cite this article: Hernández-Huerta MT, Pérez-Campos Mayoral L, Romero Díaz C, et al. Analysis of SARS-CoV-2 mutations in Mexico, Belize, and isolated regions of Guatemala and its implication in the diagnosis. *J Med Virol.* 2021;93:2099–2114. <https://doi.org/10.1002/jmv.26591>